



Published in final edited form as:

Circulation. 2016 November 15; 134(20): 1557–1567. doi:10.1161/CIRCULATIONAHA.114.014998.

Mechanical Stress Conditioning and Electrical Stimulation Promote Contractility and Force Maturation of Induced Pluripotent Stem Cell-Derived Human Cardiac Tissue

Jia-Ling Ruan, PhD¹, Nathaniel L. Tulloch, MD, PhD^{2,3}, Maria V. Razumova, PhD¹, Mark Saiget, BS³, Veronica Muskheli, MS³, Lil Pabon, PhD³, Hans Reinecke, PhD³, Michael Regnier, PhD¹, and Charles E. Murry, MD, PhD^{1,3,4}

¹Department of Bioengineering, Center for Cardiovascular Biology, Institute for Stem Cell and Regenerative Medicine, University of Washington, Seattle WA

²Department of Molecular and Cellular Biology Program, Center for Cardiovascular Biology, Institute for Stem Cell and Regenerative Medicine, University of Washington, Seattle WA

³Department of Pathology, Center for Cardiovascular Biology, Institute for Stem Cell and Regenerative Medicine, University of Washington, Seattle WA

⁴Department of Medicine/Cardiology, Center for Cardiovascular Biology, Institute for Stem Cell and Regenerative Medicine, University of Washington, Seattle WA

Abstract

Background—Tissue engineering enables the generation of functional human cardiac tissue using cells derived *in vitro* in combination with biocompatible materials. Human induced pluripotent stem cell (hiPSC)-derived cardiomyocytes provide a cell source for cardiac tissue engineering; however, their immaturity limits their potential applications. Here we sought to study the effect of mechanical conditioning and electrical pacing on the maturation of hiPSC-derived cardiac tissues.

Methods—Cardiomyocytes derived from hiPSCs were used to generate collagen-based bioengineered human cardiac tissue. Engineered tissue constructs were subjected to different mechanical stress and electrical pacing conditions.

Results—The engineered human myocardium exhibits Frank-Starling-type force-length relationships. After 2 weeks of static stress conditioning, the engineered myocardium demonstrated increases in contractility (0.63 ± 0.10 mN/mm² vs 0.055 ± 0.009 mN/mm² for no stress), tensile stiffness, construct alignment, and cell size. Stress conditioning also increased SERCA2 expression, which correlated with a less negative force-frequency relationship. When electrical pacing was combined with static stress conditioning, the tissues showed an additional

Correspondence to: Charles E. Murry, MD, PhD, Center for Cardiovascular Biology, Institute for Stem Cell and Regenerative Medicine, University of Washington, 850 Republican St, Brotman Building Rm 453, Seattle, WA 98109, Phone: 206-616-8685, Fax: 206-897-1540, murry@uw.edu and Michael Regnier, PhD, Center for Cardiovascular Biology, Institute for Stem Cell and Regenerative Medicine, University of Washington, 850 Republican St, Room S184, Seattle, WA 98109, Phone: 206-221-0504, Fax: 206-897-1540, mregnier@uw.edu.

Disclosures

None.

increase in force production (1.34 ± 0.19 mN/mm²), with no change in construct alignment or cell size, suggesting maturation of excitation-contraction coupling. Supporting this notion, we found expression of RYR2 and SERCA2 further increased by combined static stress and electrical stimulation.

Conclusions—These studies demonstrate that electrical pacing and mechanical stimulation promote maturation of the structural, mechanical and force generation properties of hiPSC-derived cardiac tissues.

Keywords

human myocardium; stress; electrical stimulation; cardiomyocyte hypertrophy; stem cell; tissue engineering

The ultimate goal of cardiac tissue engineering is to replicate functional human myocardium *in vitro*. While the target of recreating the whole heart *in vitro* remains elusive, large strides have been made towards creating contractile human cardiomyocytes and building 3 dimensional (3D) tissues that may serve as a platform for whole organ tissue engineering.^{1, 2} Functional engineered human myocardium may replace current non-human recombinant cell lines expressing cardiac ion channels for *in vitro* cardiotoxicity screening,³ may be used for disease modeling,⁴ or may be applied for regenerative purpose to treat cardiovascular diseases.⁵ Several tissue engineering approaches have recently shown promise, including scaffold free systems,⁶ engineered synthetic scaffolds,⁷ natural non-protein scaffolds,⁸ and natural protein polymers such as fibrin,^{9–15} gelatin,¹⁶ and collagen type I.^{17–26} Among them, collagen type I is attractive because it is the primary load-bearing protein in the heart which transfers the force generated by cardiomyocytes, helps maintain cardiomyocyte alignment, and provides passive tension during diastole.^{27–29}

A major limitation in cardiac tissue engineering has been a lack of a suitable human cardiomyocyte source. Obtaining cardiomyocytes directly from human hearts is not practical at the scale needed for tissue engineering. On the other hand, large numbers of cardiomyocytes can be generated from directed differentiation of human induced pluripotent stem cells (hiPSCs) or human embryonic stem cells (hESCs). These cells, however, are immature and their structure and function resemble cardiomyocytes at an early fetal stage.³⁰ Our group recently showed that hESC-derived cardiomyocytes mature to adult size and morphology within 3 months of transplantation into the infarcted hearts of non-human primates.³¹ This shows that there is no intrinsic block to maturation of these cells, so long as the correct environmental cues are provided. Studies using long term culture,^{32, 33} tri-iodothyronine (T3) hormone,³⁴ and adrenergic receptor agonists,³⁵ have proven most effective thus far in promoting maturation of human cardiomyocytes within 2D culture. For example, Shinozawa et al used *in vitro* aging to show that, while day-30 cardiomyocytes already demonstrate basic electrophysiological properties, day-60 and -90 cardiomyocytes have more mature morphological and functional traits.³⁶ On the other hand, 3D topology has been shown to influence cell morphology, cellular junctions, and myofibril protein expression.³⁷

During development, mechanical loading and electrical activity are major determinants of cardiomyocyte growth and maturation.^{38, 39} These stimuli help ensure that the heart's size

and performance are matched to the growing body's need for blood flow. This present study is aimed at examining the effects of mechanical and electrical stimulation of engineered heart tissues from hiPSCs. We report that these combined stimuli are able to promote contractility, calcium handling protein expression, and passive mechanics of the engineered human cardiac tissue.

Methods

Pluripotent Cell Culture and Cardiac Directed Differentiation

Undifferentiated human IMR90-iPSCs (James A. Thomson, U. Wisconsin-Madison) were cultured as described previously for maintenance of pluripotency (See Online Supplement for expanded Methods).²³ IRB approval for these studies was obtained in accordance with the institutional guidelines of the University of Washington. Cardiomyocytes were generated using a modified version of the monolayer-based differentiation protocol described by Laflamme et al.⁴⁰ To prepare for differentiation into cardiomyocytes, iPS cells were weaned off of mouse embryonic fibroblasts (MEFs) for 2–4 passages on Matrigel (BD Biosciences) in MEF-conditioned medium with 5 ng/mL basic FGF. To set up for differentiation, cells were passaged by Versene solution (0.5 mM EDTA and 1.1 mM glucose in PBS) and scraping with a cell lifter (Corning), followed by mild trituration with a P1000 pipette to attain a mostly single cell suspension for even replating. Cells were then plated into Matrigel-coated 24-well plates (Corning) at a density of 300,000 cells per well in 1 mL of MEF-conditioned medium with 5 ng/mL basic FGF. Medium was changed daily until the plates had attained confluence with a packed-in morphology (24–48 hours from plating). One day before the initiation of differentiation, the cells were incubated with medium supplemented with 1 μ M Chiron 9902 (a Wnt agonist, Cayman). Differentiation was initiated by feeding the cells with 0.5 mL of RPMI medium (Invitrogen) containing B27 supplement without insulin (Invitrogen), 100 U/mL penicillin G, 100 mg/mL streptomycin, and 100 ng/mL activin A (R&D Systems). After 24 hours, medium was carefully changed to 1 mL of the same medium containing no activin A and supplemented with 5 ng/mL BMP4 (R&D Systems) and 1 μ M Chiron 9902. At day 3 of differentiation, plates were fed with 1 mL of the same medium supplemented with 1 μ M Xav 939 (a Wnt antagonist, Tocris Bioscience). Plates were then fed every other day with 1 mL of the same medium without Xav 939 after day 5. Spontaneously contracting cardiomyocytes were observed beginning day 8 to day 12 from the onset of differentiation. Cardiomyocyte preparations were used for generation of cardiac constructs between day 14 and day 21 from onset of differentiation, and at the time of construct generation, moved into RPMI medium made with standard B27 supplement containing insulin (Invitrogen).

Generation of Cardiac Constructs

To make engineered heart tissue constructs, hiPSC-derived cardiomyocytes were trypsinized into single cells from Matrigel plates and then encapsulated in a collagen-based 3D scaffold as described previously (See Online Supplement for expanded Methods).²³ The cell/gel mixture (2 million cells per 100 μ L of collagen gel) was casted into trough in Tissue Train 6-well plates (Flexcell). After 1 hour at room temperature for matrix solidification, the base-plate vacuum was released and the resulting cardiac tissue constructs were placed into RPMI

medium with standard B27 supplement containing insulin. One day after construct generation, cell viability was analyzed by LIVE/DEAD staining kit (Life Technology) with 30-minute incubation with dyes and then imaging under a fluorescent microscope. Static stress conditioning was achieved by maintaining constructs at a fixed static length, whereas no stress conditions were achieved with one end of the construct cut free of the nylon tab. Constructs were maintained in a regimen of no stress or static stress conditioning for a period of 2 weeks before analysis. For combined mechanical and electrical stimulation, 1-week static stress conditioned constructs were subjected to a second week of electrical stimulation with 2 Hz, 5 Volt/cm, 5 ms pulse (C-Pace EP Culture Pacer, IonOptix). The three stimulation conditions are referred as no stress (NS), static stress (SS), and static stress + E pacing (SE). For analysis of cardiomyocyte input purity, a subset of cells used for construct generation was quantified by flow cytometry for cardiac troponin T (cTnT) expression (See Online Supplement for expanded Methods). The average cardiac troponin T (cTnT) positive portion was $73\pm 3\%$ from 9 runs of differentiation (Figure 1A).

Mechanical Measurements

The experimental setup is shown schematically in Supplement Figure 1. Constructs (dimension at seeding $\sim 20\times 1\times 1$ mm, thickness at time of measurement ~ 0.3 mm) were carefully dissected into 2 mm-long sections and then suspended on stainless steel hooks attached to a force transducer (Aurora Scientific, model 400A) and a length controller (Aurora Scientific, model 312B). Slack length was determined as the length immediately preceding the stretch step that led to a positive amplitude twitch transient on the force trace. Force of spontaneously contracting constructs was continuously monitored as preparation length was changed by adjusting the position of the length controller arm. For cell-free collagen matrix constructs, slack length was set to the length at which a 4% stretch step resulted in an immediate increase in measured passive force. From the initial slack length, 4% stretches were made at intervals of 30 seconds each to a final length of 125% initial length. Force and length signals were digitally recorded and analyzed using custom LabView software. Passive tension and the amplitude of spontaneous isometric twitch force were measured on 4 consecutive transients in the plateau region after each length step. Force was normalized to cross-sectional area of the preparation, calculated by measuring the diameter at non-strained length and assuming circular cross-sectional geometry. For force-frequency relation studies, constructs were paced at 2, 2.5, and 3 Hz, using pulses of 5 volts/cm with 40 ms pulse duration. An inline perfusion system (Warner Instruments) was used to keep the solution temperature at 37°C and infuse drugs. The twitch force amplitudes were measured on 4 transients at each frequency. Constructs were perfused with HEPES-buffered Tyrode solution (pH 7.4; 1.8 mM calcium unless indicated otherwise). $N=6$ for NS, $n=7$ for SS, and $n=9$ for ES. Contractile responses were determined under the following conditions: varying extracellular Ca^{2+} from 10–4000 μM , 1 μM verapamil (Tocris Bioscience), and 1 μM Bay K8644 (Tocris Bioscience).

Immunostaining, Microscopy and Histological Analysis

Detail of immunostaining and microscopy are described within the online expanded Methods section. For measurements of cell/collagen alignment and cell volume fraction in constructs, slides were stained with Sirius Red/Fast Green. For cell size measurement and

bona fide muscle cross sectional area study, slides were stained with MYH7 antibody and anti- α -actinin, respectively. For immunofluorescence, slides were stained with the primary antibody or a cocktail of two primary antibodies overnight at 4 °C, followed by one hour with an Alexa fluorophore-conjugated secondary antibody or a cocktail of two secondary antibodies with incubation for one hour at room temperature. Hoechst 33342 (Sigma) counterstain was used to visualize the nuclei. To quantify alignment within the constructs, Sirius Red/Fast Green stained micrographs were taken by either a light microscope or a polarized microscope and analyzed using a custom fiber orientation analysis program as previously described.²³ Alignment is defined by the inverse of the magnitude of angle dispersion (the standard deviation of angles of cell edges). Low angle dispersion indicates high degree of alignment. For cell volume fraction analysis, Sirius Red and Fast Green channels were separated by color deconvolution plugin in ImageJ (NIH)⁴¹ and converted into grey scale images. The cell volume fraction (percentage cell area within the construct) was defined by the Fast Green positive area divided by the total construct area. To quantify cell size, 400X MYH7 stained micrographs were analyzed by dividing the DAB positive area by the number of DAB-positive cells in the area. 100X α -actinin stained images were used to quantify bone fide muscle cross sectional area.

Western Blot and Calcium Transient Analysis

Western blot and calcium transient study were performed as described in the expanded Methods section. For western blots, all proteins were normalized to GAPDH expression level (n=8 for NS, n=7 for SS, and n=7 for SE in total for three runs of biologically independent experiments).

Statistical Analysis

Results are given as the mean \pm standard error of the mean (SEM); error bars within graphs also represent SEM. Significance was determined using Kruskal-Wallis test and pairwise p value was calculated by Mann-Whitney test with 95% or greater confidence level based on Bonferroni correction for multiple comparisons. Friedman's test was used to analyze the force-frequency data set and the adjusted p value from Dunn's multiple comparisons test was reported. To reduce inter-experimental variation between western blot films, in some experiments western blot data were log-transformed, mean-centered, and then autoscaled as described previously.⁴² A p value <0.05 was considered statistically significant.

Results

Generation of Engineered hiPSC-Derived Cardiac Tissue

Using a monolayer-based direct differentiation protocol (see Methods), we are able to generate high purity of cardiomyocytes from human induced pluripotent stem cells (73 \pm 3% cTnT+ cells based on flow cytometry; Figure 1A). The hiPSC-derived cardiomyocytes displayed nuclear expression of the cardiomyocyte transcription factor Nkx2.5 and robust sarcomeric organization visualized by α -actinin immunostaining (Figure 1B). Cardiac tissue constructs were created by embedding the cardiomyocyte preparation into a collagen-based scaffold.^{23, 26} Over 70% of cells were still viable after 24 hour of cell seeding (71.2 \pm 3.6%). The engineered constructs were then subjected to 2 weeks of culture under conditions of no

mechanical stress (NS; one end cut free from the attachment tab), 2 weeks of static stress (SS), or 2 weeks of static stress including 1 week of electrical pacing (SE). Spontaneous contraction was generally observed by 4 to 7 days post-construct formation for all groups. After 2 weeks of growth and remodeling, we observed many primitive intercalated disc-like structures containing stress-transmitting fascia adherens junctions and desmosomes by TEM (Figure 1C and Supplement Figure 2). In addition, engineered constructs subjected to SS (Figure 1E) and SE (Figure 1F) exhibited improved cardiomyocyte density and myofibrillar alignment (visualized using cTnT immunostaining) when compared to NS constructs (Figure 1D).

Structural Remodeling and Cardiac Hypertrophy of Engineered Cardiac Tissues

We quantified the intercellular alignment by measuring the reciprocal of the cell axis dispersion angles.²³ Both the SS and SE groups showed higher degree of alignment compared to NS group (Figure 2A, alignment value of SS: 4.39 ± 0.57 , SE: 4.08 ± 0.37 , NS: 1.17 ± 0.06 , NS vs SS, $p=0.0006$; NS vs SE, $p=0.006$). However, pacing along with stress conditioning did not further promote cell alignment over stress alone (SS vs SE, $p=0.5$). To understand how conditioning affects tissue stiffness, we measured passive force from human cardiac constructs using a series of short increasing length steps while simultaneously recording diastolic tension (Figure 2B). Cell-free collagen matrix constructs have a passive stiffness of 0.079 ± 0.041 kPa, while constructs with cardiomyocytes in the NS condition demonstrated a passive stiffness of 0.47 ± 0.22 kPa, which is not significantly different from the cell free constructs. SS conditioning significantly promotes the passive stiffness markedly to 11.13 ± 1.17 kPa, while the combination with SE conditioning raised passive stiffness about two-fold further to 21.51 ± 4.02 kPa (collagen vs SS, $p=0.006$; collagen vs SE, $p=0.003$; NS vs SS, $p=0.001$; NS vs SE, $p=0.0004$; SS vs SE, $p=0.03$). This change in stiffness is correlated with an increase in cell volume fraction from $39.9 \pm 2.5\%$ in NS to $53.1 \pm 4.3\%$ in SS and $63.2 \pm 6.3\%$ in SE (Figure 2C, NS vs SE, $p=0.01$; NS vs SS, $p=0.07$). A higher collagen alignment was also observed from NS to SS and SE groups (Supplement Figure 3, alignment value of SS: 2.18 ± 0.31 , SE: 2.26 ± 0.29 , NS: 1.38 ± 0.12 , NS vs SS, $p=0.03$, NS vs SE, $p=0.03$). On the other hand, there was no significant increase from SS to SE groups in terms of cell volume fraction and construct alignment.

We assessed the size of cardiomyocytes by quantifying the MYH7 area within the construct (Figure 3). Cardiomyocytes within constructs exposed to SS ($774 \pm 38 \mu\text{m}^2$) are significantly larger than those in the NS condition ($503 \pm 26 \mu\text{m}^2$). Combination of static stress with electrical pacing did not result in a further increase in cardiomyocyte size compared to SS-conditioned group alone ($795 \pm 46 \mu\text{m}^2$). We also quantified the bona fide muscle cross sectional area by analyzing α -actinin positive area in cross section within engineered tissues and did not find any difference among different stimulation conditionings (NS: $21.0 \pm 4.63\%$, SS: $23.13 \pm 3.99\%$, SE: $28.60 \pm 7.01\%$).

Contractility of Engineered Heart Tissues

We examined active twitch force recorded over an incrementally lengthening stretch routine (Figure 4A). As can be observed in the force trace example in Figure 4B, active twitch force transients, undistinguishable at slack length, appeared and increased in amplitude over a

series of 4% lengthening stretches, in accordance with the cellular basis of the Frank-Starling mechanism. These spontaneous twitch force transients disappeared upon incubation with 2,3-butanedione monoxime (BDM, 30 mM), a reversible inhibitor of actin-myosin interaction (Supplement Figure 4A, 4B), but reappeared upon washout (Supplement Figure 4C). Incubation with the β -adrenergic agonist isoproterenol markedly increased the rate of spontaneous contractions but did not significantly increase force (Supplement Figure 4D). The amplitude of active force production in the engineered cardiac tissue changed with extracellular calcium concentration (Supplement Figure 5A). The L-type calcium channel inhibitor verapamil reduced the twitch force amplitude (Supplement Figure 5B and 5C) while L-type calcium channel agonist, Bay K8644, increased the contraction rate and slightly increased force amplitude (Supplement Figure 5D and 5E). These experiments demonstrate a key role for extracellular calcium in driving the contractile function. We then generated Starling curves by plotting the amplitude of twitch force, normalized to cross-sectional area, versus change in length (Figure 4C). A comparison of the slopes of this relationship illustrates the difference in contractility of these constructs (Figure 4D). We observed a more than 10-fold enhancement in contractility comparing NS to SS conditioning ($p=0.0012$). Adding electrical pacing further augmented contractility by additional 2-fold (SS vs SE, $p=0.0164$).

Calcium Handling of Bioengineered Cardiac Tissue

We hypothesized that the enhancement in contractility results at least partially from maturation of excitation-contraction coupling of the engineered tissues. Western blots demonstrated that SERCA2 protein expression was upregulated 2-fold by SS conditioning (NS vs SS, $p=0.0037$). SE also exhibited a 2.5-fold increase from NS conditioning (NS vs SE, $p=0.0006$). However, addition of electrical pacing did not reach significance in SERCA2 expression when comparing to SS conditioning (Figure 5B). RYR2 expression in SE group was also elevated by 1.5-fold from NS conditioning but only slightly increased from SS conditioning (Figure 5C). To normalize the variability between western blot experiments, band intensities were also standardized by log-transforming, mean-centering, and autoscaling.⁴² SERCA2 expression from standardized data showed similar enhancement from NS to SS and NS to SE like raw data (Supplement Figure 6A), while significant increase of RYR2 expression from NS to SS or SE was revealed in the standardized dataset (Supplement Figure 6B, NS vs SS, $p=0.0132$, NS vs SE, $p=0.0025$). Using calcium flux dye, we examined the conduction velocity of the tissue constructs, estimated from the Ca^{2+} propagation wave, and demonstrated an average speed of 2.76 ± 0.61 cm/s at 30 °C with no significant difference between groups.

We then examined the force-frequency relationship, a well-established maturation index for excitation-contraction coupling. Adult human cardiomyocytes have a positive force-frequency relationship, showing increasing force with increasing pacing frequency, while human stem cell-derived cardiomyocytes have a negative force-frequency relationship,⁴³ likely due to immature sarcoplasmic reticulum (SR), such that increased pacing frequency reduces active force production. In the NS engineered heart tissues we found a prominently negative force-frequency relationship. As stimulation frequency increased from 2 to 3 Hz, twitch amplitude significantly decreased by $43.19 \pm 0.01\%$ ($p=0.0047$). In tissues conditioned

by SS, however, twitch amplitude showed a non-significant decrease of $16.8 \pm 0.03\%$ from 2 to 3 Hz ($p=0.1$). The tissues conditioned by SE showed a $4.4 \pm 0.4\%$ decrease in force production from 2 to 3 Hz, barely changed from baseline (Figure 6A, $p=0.87$). These data demonstrate a more mature dynamic balance of calcium handling in the SS and, especially, SE conditioned constructs.

Discussion

In the current study we demonstrated that human myocardium can be generated using hiPSCs, and that this engineered heart tissue is highly responsive to both mechanical and electrical cues. In response to static stress, the engineered heart tissues showed increased cell alignment, cardiomyocyte hypertrophy, increased contractility and passive stiffness, increased expression of Ca^{2+} handling proteins, and an improvement in the force-frequency relationship for immature cardiomyocytes. When electrical pacing was added to the conditioning regimen, we observed a further increase in passive stiffness and cell volume fraction, an additional 2-fold increase in contractility, further increased expression of Ca^{2+} handling proteins and a less negative force-frequency relation.

Previous observations have estimated the size of hESC-derived cardiomyocytes, cultured on monolayer, to be $480 \pm 32 \mu\text{m}^2$ in the early stages (day 20–40 post differentiation) and revealed that longer term culture (80–120 days post differentiation) is needed to increase the size 3-fold.³³ Here, our input population used cardiomyocytes from day 14–21 post differentiation and, after the additional 14 day of tissue culture conditioning, the cardiomyocytes are still early stage (less than day 40 post differentiation). With stress conditioning in the construct, early stage hiPSC-derived cardiomyocytes demonstrated a 1.5-fold increase in size. SE conditioning showed a trend toward further cardiac hypertrophy, but not to significance. Similar cell size increases have been observed with T3-treatment of early stage hiPSC-derived cardiomyocytes in 2D culture with a 1.5-fold size increase in a 1-week treatment.³⁴

Compared to embryoid body or monolayer culture of cardiomyocytes, 3D engineered heart tissue shows significant cellular maturation.^{11, 15, 18, 24} Our previous study showed that cyclic stress and SS demonstrate comparable effects in structural organization of pluripotent stem cell-derived cardiac constructs.²³ Here we showed that the SS conditioning enhances the contractile function of engineered myocardium, which has not been demonstrated in previous studies.^{10, 23, 24, 44} Electrical pacing does not promote obvious structural maturation compared to the SS-treated group, but electrical pacing does enhance the contractility of the engineered tissue. Overall, the passive stiffness of these constructs is still less than that of rat neonatal myocardium ($38.5 \pm 9.1 \text{ kPa}$).⁴⁵ This could result from lower cell alignment in engineered cardiac tissue compared to naïve myocardium (cell alignment value of rat heart is ~ 9.08).^{23, 46, 47}

The relative immaturity of this engineered myocardium is also reflected in the low force development compared to native myocardium, where active force from human adult ventricular strip is generally over 10 mN/mm^2 .^{46, 47} Our engineered cardiac tissues showed force production within the range of most reported values using neonatal rat ventricular

myocytes (0.4–4.6 mN/mm²) or human stem cell-derived cardiomyocytes (0.12–4.4 mN/mm²).^{11, 24, 25, 48} It should be noted that the methods to calculate the contractile force amplitude are not standardized among research groups. For example, variation in the myocyte volume fraction or the percent of non-myocytes may influence the overall tissue force development. Additionally many studies just report the absolute force generated by constructs, but differences between studies in tissue geometry make it difficult to compare the results. By analyzing α -actinin positive area within the cross section of our constructs, we show that there is no difference in bona fide muscle cross sectional area between three conditioning groups (NS: 21.0±4.63%, SS: 23.13±3.99%, SE: 28.60±7.01%). Thus, the twitch forces normalized with cell-based cross sectional area at 125 % stretch for NS, SS, and SE are 0.08, 0.83, 1.30 mN/mm², respectively, which are close to the active force production from newborn (1.1 ±0.3 mN/mm² at 2 Hz pacing) and infant strip (1.7±0.9 mN/mm² at 2 Hz pacing).⁴⁹

An important observation in this study was that our engineered heart tissue constructs demonstrated increasing twitch force as length increases, in accordance with the cellular basis of the Frank-Starling mechanism. This is a fundamental characteristic of native heart muscle, and its presence here suggests we are on the right track in developing realistic models of human myocardium. Several studies have demonstrated similar results anecdotally in human stem cell-derived cardiac tissue,^{15, 17, 23, 24} but in this current study, we demonstrated this effect in hiPSC-derived myocardium and, further, established that contractility can be promoted by combining electrical and mechanical conditioning. Indeed, length-dependent contractility was increased 2-fold in the SE group compared to the SS-conditioned tissues, and the SS group demonstrated at least 10-fold enhancement over NS group. The increased contractility likely has several components, including greater cell/collagen alignment as well as cardiomyocyte hypertrophy, and increased expression of Ca²⁺ handling proteins such as SERCA2 and RYR2. This maturation of the SR was associated with improvements in the negative force-frequency relationship.

It was interesting that electrical pacing had an additive effect on passive stiffness (>2-fold increase), contractility (>2-fold increase), and expression of calcium handling proteins (1.5–2.5-fold increase), without having detectable effects on cell alignment or size. This indicates that different features of maturation are controlled by different stimuli and suggests that multiple pathways may be needed for optimal maturation. One caveat to our experiments is that longer electrical stimulation periods or different stimulation regimes may be needed to further promote this effect. For instance, studies by Hirt et al indicated that chronic electrical pacing for 16–18 days promoted higher cardiomyocyte to ECM ratio.¹⁰ Additionally, Nunes et al also showed that a gradually increasing pacing frequency from 1–6 Hz over a week can further enhance the structure and electrophysiological function of engineered cardiac constructs compared to a low frequency ramp up regime from 1–3 Hz.¹⁸

In summary, we generated cardiac tissue from hiPSC-derived cardiomyocytes and demonstrated structural and functional improvement of this bioengineered myocardium when subjected to stress conditioning and electrical stimulation. Specifically, we show that: 1) 2-week stress conditioning promotes alignment, passive stiffness, cardiac hypertrophy, and contractility of engineered cardiac tissues, 2) the contractility of engineered cardiac

tissues can be further promoted by 1-week electrical stimulation, and 3) the enhancement in functional maturation from these cues is correlated to the enhanced expression of SR-related proteins.

Through these studies, we are able to link relationships between conditional cues and functional response in developing human myocardium. The implications of these results are two-fold: we begin to understand maturation cues in the developing human heart, and we also begin to build a bioengineering toolbox for the development of more clinically relevant engineered tissues. With these tools, we can now work towards the complementary objectives of 1) generating more mature patient-derived iPSC-based tissue for eventual clinical cardiac therapy and 2) determining relationships between calcium handling and force production in the pathogenesis of human cardiomyopathies using engineered human cardiac tissues from normal and myopathic patient lines.

Supplementary Material

Refer to Web version on PubMed Central for supplementary material.

Acknowledgments

We thank Dr. Michael Laflamme for advice on improving differentiation, and Dr. Carol Ware and Ms. Angel Nelson from the Ellison Stem Cell Core in the Institute for Stem Cell & Regenerative Medicine for their expertise and assistance in freezing, thawing, and maintaining pluripotent stem cells. We also thank Dr. James Thomson for the kind use of their iPSC cell line. We thank Dr. Steven Korte for the assistance in calcium transient studies. We thank Drs. Wei-Zhong Zhu and Michael Laflamme for kindly sharing the antibodies for immunohistology and Western blotting.

Sources of Funding

This work was supported by NIH grants R01HL084642, R01HL111197, P01HL094374, U01HL100405, P01GM081619, and a grant from the Fondation Leducq Transatlantic Network of Excellence. NLT was supported by T32HL007312 and T32GM007266.

References

1. Ogle BM, Bursac N, Domian I, Huang NF, Menasche P, Murry CE, Pruitt B, Radisic M, Wu JC, Wu SM, Zhang J, Zimmermann WH, Vunjak-Novakovic G. Distilling complexity to advance cardiac tissue engineering. *Sci Transl Med*. 2016; 8:342ps13.
2. Jackman CP, Shadrin IY, Carlson AL, Bursac N. Human Cardiac Tissue Engineering: From Pluripotent Stem Cells to Heart Repair. *Curr Opin Chem Eng*. 2015; 7:57–64. [PubMed: 25599018]
3. Kurokawa YK, George SC. Tissue engineering the cardiac microenvironment: Multicellular microphysiological systems for drug screening. *Adv Drug Deliv Rev*. 2016; 96:225–33. [PubMed: 26212156]
4. Tzatzalos E, Abilez OJ, Shulda P, Wu JC. Engineered heart tissues and induced pluripotent stem cells: Macro- and microstructures for disease modeling, drug screening, and translational studies. *Advanced Drug Delivery Reviews*. 2016; 96:234–244. [PubMed: 26428619]
5. Feric NT, Radisic M. Strategies and Challenges to Myocardial Replacement Therapy. *Stem Cells Translational Medicine*. 2016; 5:410–416. [PubMed: 26933042]
6. Kreutziger KL, Muskheli V, Johnson P, Braun K, Wight TN, Murry CE. Developing Vasculature and Stroma in Engineered Human Myocardium. *Tissue Engineering Part A*. 2011; 17:1219–1228. [PubMed: 21187004]

7. Madden LR, Mortisen DJ, Sussman EM, Dupras SK, Fugate JA, Cuy JL, Hauch KD, Laflamme MA, Murry CE, Ratner BD. Proangiogenic scaffolds as functional templates for cardiac tissue engineering. *Proceedings of the National Academy of Sciences*. 2010; 107:15211–15216.
8. Dar A, Shachar M, Leor J, Cohen S. Optimization of cardiac cell seeding and distribution in 3D porous alginate scaffolds. *Biotechnol Bioeng*. 2002; 80:305–312. [PubMed: 12226863]
9. Birla RK, Huang YC, Dennis RG. Development of a Novel Bioreactor for the Mechanical Loading of Tissue-Engineered Heart Muscle. *Tissue Engineering*. 2007; 13:2239–2248. [PubMed: 17590151]
10. Hirt MN, Boeddinghaus J, Mitchell A, Schaaf S, Börnchen C, Müller C, Schulz H, Hubner N, Stenzig J, Stoehr A, Neuber C, Eder A, Luther PK, Hansen A, Eschenhagen T. Functional improvement and maturation of rat and human engineered heart tissue by chronic electrical stimulation. *Journal of Molecular and Cellular Cardiology*. 2014; 74:151–161. [PubMed: 24852842]
11. Schaaf S, Shibamiya A, Mewe M, Eder A, Stöhr A, Hirt MN, Rau T, Zimmermann W-H, Conradi L, Eschenhagen T, Hansen A. Human Engineered Heart Tissue as a Versatile Tool in Basic Research and Preclinical Toxicology. *PLoS ONE*. 2011; 6:e26397. [PubMed: 22028871]
12. Liao B, Christoforou N, Leong KW, Bursac N. Pluripotent stem cell-derived cardiac tissue patch with advanced structure and function. *Biomaterials*. 2011; 32:9180–9187. [PubMed: 21906802]
13. Thomson KS, Korte FS, Giachelli CM, Ratner BD, Regnier M, Scatena M. Prevascularized Microtemplated Fibrin Scaffolds for Cardiac Tissue Engineering Applications. *Tissue Engineering Part A*. 2013; 19:967–977. [PubMed: 23317311]
14. Thomson KS, Dupras SK, Murry CE, Scatena M, Regnier M. Proangiogenic microtemplated fibrin scaffolds containing aprotinin promote improved wound healing responses. *Angiogenesis*. 2013; 17:195–205. [PubMed: 24127199]
15. Zhang D, Shadrin IY, Lam J, Xian H-Q, Snodgrass HR, Bursac N. Tissue-engineered cardiac patch for advanced functional maturation of human ESC-derived cardiomyocytes. *Biomaterials*. 2013; 34:5813–5820. [PubMed: 23642535]
16. Mihic A, Li J, Miyagi Y, Gagliardi M, Li S-H, Zu J, Weisel RD, Keller G, Li R-K. The effect of cyclic stretch on maturation and 3D tissue formation of human embryonic stem cell-derived cardiomyocytes. *Biomaterials*. 2014; 35:2798–2808. [PubMed: 24424206]
17. Turnbull IC, Karakikes I, Serrao GW, Backeris P, Lee JJ, Xie C, Senyei G, Gordon RE, Li RA, Akar FG, Hajjar RJ, Hulot JS, Costa KD. Advancing functional engineered cardiac tissues toward a preclinical model of human myocardium. *The FASEB Journal*. 2013; 28:644–654. [PubMed: 24174427]
18. Nunes SS, Miklas JW, Liu J, Aschar-Sobbi R, Xiao Y, Zhang B, Jiang J, Massé S, Gagliardi M, Hsieh A, Thavandiran N, Laflamme MA, Nanthakumar K, Gross GJ, Backx PH, Keller G, Radisic M. Biowire: a platform for maturation of human pluripotent stem cell-derived cardiomyocytes. *Nature Methods*. 2013; 10:781–787. [PubMed: 23793239]
19. Zimmermann WH, Didie M, Wasmeier GH, Nixdorff U, Hess A, Melnychenko I, Boy O, Neuhuber WL, Weyand M, Eschenhagen T. Cardiac grafting of engineered heart tissue in syngenic rats. *Circulation*. 2002; 106:1151–7. [PubMed: 12354725]
20. Thavandiran N, Dubois N, Mikryukov A, Masse S, Beca B, Simmons CA, Deshpande VS, McGarry JP, Chen CS, Nanthakumar K, Keller GM, Radisic M, Zandstra PW. Design and formulation of functional pluripotent stem cell-derived cardiac microtissues. *Proceedings of the National Academy of Sciences*. 2013; 110:E4698–E4707.
21. Shimko VF, Claycomb WC. Effect of Mechanical Loading on Three-Dimensional Cultures of Embryonic Stem Cell-Derived Cardiomyocytes. *Tissue Engineering Part A*. 2008; 14:49–58. [PubMed: 18333804]
22. Zimmermann W-H, Melnychenko I, Wasmeier G, Didié M, Naito H, Nixdorff U, Hess A, Budinsky L, Brune K, Michaelis B, Dhein S, Schwöerer A, Ehmke H, Eschenhagen T. Engineered heart tissue grafts improve systolic and diastolic function in infarcted rat hearts. *Nature Medicine*. 2006; 12:452–458.

23. Tulloch NL, Muskheli V, Razumova MV, Korte FS, Regnier M, Hauch KD, Pabon L, Reinecke H, Murry CE. Growth of Engineered Human Myocardium With Mechanical Loading and Vascular Coculture. *Circulation Research*. 2011; 109:47–59. [PubMed: 21597009]
24. Kensah G, Roa Lara A, Dahlmann J, Zweigerdt R, Schwanke K, Hegermann J, Skvorc D, Gawol A, Azizian A, Wagner S, Maier LS, Krause A, Drager G, Ochs M, Haverich A, Gruh I, Martin U. Murine and human pluripotent stem cell-derived cardiac bodies form contractile myocardial tissue in vitro. *European Heart Journal*. 2012; 34:1134–1146. [PubMed: 23103664]
25. Kensah G, Gruh I, Viering J, Schumann H, Dahlmann J, Meyer H, Skvorc D, Bär A, Akhyari P, Heisterkamp A, Haverich A, Martin U. A Novel Miniaturized Multimodal Bioreactor for Continuous In Situ Assessment of Bioartificial Cardiac Tissue During Stimulation and Maturation. *Tissue Engineering Part C: Methods*. 2011; 17:463–473. [PubMed: 21142417]
26. Zimmermann WH, Schneiderbanger K, Schubert P, Didie M, Munzel F, Heubach JF, Kostin S, Neuhuber WL, Eschenhagen T. Tissue engineering of a differentiated cardiac muscle construct. *Circ Res*. 2002; 90:223–30. [PubMed: 11834716]
27. Fomovsky GM, Thomopoulos S, Holmes JW. Contribution of extracellular matrix to the mechanical properties of the heart. *Journal of Molecular and Cellular Cardiology*. 2010; 48:490–496. [PubMed: 19686759]
28. Granzier HL, Irving TC. Passive tension in cardiac muscle: contribution of collagen, titin, microtubules, and intermediate filaments. *Biophysical Journal*. 1995; 68:1027–1044. [PubMed: 7756523]
29. Vunjak Novakovic G, Eschenhagen T, Mummery C. Myocardial Tissue Engineering: In Vitro Models. *Cold Spring Harbor Perspectives in Medicine*. 2014; 4:a014076–a014076. [PubMed: 24591534]
30. Yang X, Pabon L, Murry CE. Engineering Adolescence: Maturation of Human Pluripotent Stem Cell-Derived Cardiomyocytes. *Circulation Research*. 2014; 114:511–523. [PubMed: 24481842]
31. Chong JJH, Yang X, Don CW, Minami E, Liu Y-W, Weyers JJ, Mahoney WM, Van Biber B, Cook SM, Palpant NJ, Gantz JA, Fugate JA, Muskheli V, Gough GM, Vogel KW, Astley CA, Hotchkiss CE, Baldessari A, Pabon L, Reinecke H, Gill EA, Nelson V, Kiem H-P, Laflamme MA, Murry CE. Human embryonic-stem-cell-derived cardiomyocytes regenerate non-human primate hearts. *Nature*. 2014; 510:273–277. [PubMed: 24776797]
32. Kamakura T, Makiyama T, Sasaki K, Yoshida Y, Wuriyanghai Y, Chen J, Hattori T, Ohno S, Kita T, Horie M, Yamanaka S, Kimura T. Ultrastructural Maturation of Human-Induced Pluripotent Stem Cell-Derived Cardiomyocytes in a Long-Term Culture. *Circulation Journal*. 2013; 77:1307–1314. [PubMed: 23400258]
33. Lundy SD, Zhu W-Z, Regnier M, Laflamme MA. Structural and Functional Maturation of Cardiomyocytes Derived from Human Pluripotent Stem Cells. *Stem Cells and Development*. 2013; 22:1991–2002. [PubMed: 23461462]
34. Yang X, Rodriguez M, Pabon L, Fischer KA, Reinecke H, Regnier M, Sniadecki NJ, Ruohola-Baker H, Murry CE. Tri-iodo-L-thyronine promotes the maturation of human cardiomyocytes-derived from induced pluripotent stem cells. *Journal of Molecular and Cellular Cardiology*. 2014; 72:296–304. [PubMed: 24735830]
35. Földes G, Mioulane M, Wright JS, Liu AQ, Novak P, Merkely B, Gorelik J, Schneider MD, Ali NN, Harding SE. Modulation of human embryonic stem cell-derived cardiomyocyte growth: A testbed for studying human cardiac hypertrophy? *Journal of Molecular and Cellular Cardiology*. 2011; 50:367–376. [PubMed: 21047517]
36. Shinozawa T, Imahashi K, Sawada H, Furukawa H, Takami K. Determination of Appropriate Stage of Human-Induced Pluripotent Stem Cell-Derived Cardiomyocytes for Drug Screening and Pharmacological Evaluation In Vitro. *Journal of Biomolecular Screening*. 2012; 17:1192–1203. [PubMed: 22706346]
37. Soares CP, Midlej V, Oliveira MEWd, Benchimol M, Costa ML, Mermelstein C. 2D and 3D-Organized Cardiac Cells Shows Differences in Cellular Morphology, Adhesion Junctions, Presence of Myofibrils and Protein Expression. *PLoS ONE*. 2012; 7:e38147. [PubMed: 22662278]
38. Lasher RA, Pahnke AQ, Johnson JM, Sachse FB, Hitchcock RW. Electrical stimulation directs engineered cardiac tissue to an age-matched native phenotype. *Journal of Tissue Engineering*. 2012;3.

39. Ruwhof C. Mechanical stress-induced cardiac hypertrophy: mechanisms and signal transduction pathways. *Cardiovascular Research*. 2000; 47:23–37. [PubMed: 10869527]
40. Laflamme MA, Chen KY, Naumova AV, Muskheli V, Fugate JA, Dupras SK, Reinecke H, Xu C, Hassanipour M, Police S, O'Sullivan C, Collins L, Chen Y, Minami E, Gill EA, Ueno S, Yuan C, Gold J, Murry CE. Cardiomyocytes derived from human embryonic stem cells in pro-survival factors enhance function of infarcted rat hearts. *Nat Biotechnol*. 2007; 25:1015–1024. [PubMed: 17721512]
41. Ruifrok AC, Katz RL, Johnston DA. Comparison of Quantification of Histochemical Staining By Hue-Saturation-Intensity (HSI) Transformation and Color-Deconvolution. *Applied Immunohistochemistry & Molecular Morphology*. 2003; 11:85–91. [PubMed: 12610362]
42. Willems E, Leyns L, Vandesompele J. Standardization of real-time PCR gene expression data from independent biological replicates. *Analytical Biochemistry*. 2008; 379:127–129. [PubMed: 18485881]
43. Germanguz I, Sedan O, Zeevi-Levin N, Shtrichman R, Barak E, Ziskind A, Eliyahu S, Meiry G, Amit M, Itskovitz-Eldor J, Binah O. Molecular characterization and functional properties of cardiomyocytes derived from human inducible pluripotent stem cells. *Journal of Cellular and Molecular Medicine*. 2009; 15:38–51.
44. Fink C, Ergun S, Kralisch D, Remmers U, Weil J, Eschenhagen T. Chronic stretch of engineered heart tissue induces hypertrophy and functional improvement. *FASEB J*. 2000; 14:669–79. [PubMed: 10744624]
45. Moreno-Gonzalez A, Korte FS, Dai J, Chen K, Ho B, Reinecke H, Murry CE, Regnier M. Cell therapy enhances function of remote non-infarcted myocardium. *Journal of Molecular and Cellular Cardiology*. 2009; 47:603–613. [PubMed: 19683533]
46. Holubarsch C. Shortening versus isometric contractions in isolated human failing and non-failing left ventricular myocardium: dependency of external work and force on muscle length, heart rate and inotropic stimulation. *Cardiovascular Research*. 1998; 37:46–57. [PubMed: 9539857]
47. Mulieri LA, Hasenfuss G, Leavitt B, Allen PD, Alpert NR. Altered myocardial force-frequency relation in human heart failure. *Circulation*. 1992; 85:1743–1750. [PubMed: 1572031]
48. Leontyev S, Schlegel F, Spath C, Schmiedel R, Nichtitz M, Boldt A, Rübsamen R, Salameh A, Kostelka M, Mohr F-W, Dhein S. Transplantation of engineered heart tissue as a biological cardiac assist device for treatment of dilated cardiomyopathy. *European Journal of Heart Failure*. 2013; 15:23–35. [PubMed: 23243122]
49. Wiegerinck RF, Cojoc A, Zeidenweber CM, Ding G, Shen M, Joyner RW, Fernandez JD, Kanter KR, Kirshbom PM, Kogon BE, Wagner MB. Force Frequency Relationship of the Human Ventricle Increases During Early Postnatal Development. *Pediatr Res*. 2009; 65:414–419. [PubMed: 19127223]

Clinical Perspective

What's new?

- Tissue engineering, in conjunction with human induced pluripotent stem cells and protocols to differentiate them towards the cardiac lineage, holds great promise for clinical applications, drug testing and disease modeling.
- However, the stem cell-derived human cardiomyocytes are still quite immature and do not reflect the adult phenotype.
- Here, we show that mechanical and electrical stimulation promote maturation of the molecular, structural, force-generation properties of human induced pluripotent stem cell-derived cardiac tissues.

What are the clinical implications?

- Through these studies, we are able to link relationships between biophysical cues, e.g. mechanical load and heart rate, and functional response in developing human myocardium.
- We begin to understand maturation cues in the developing human heart.
- We are building a bioengineering toolbox for the development of more clinically relevant engineered tissues.

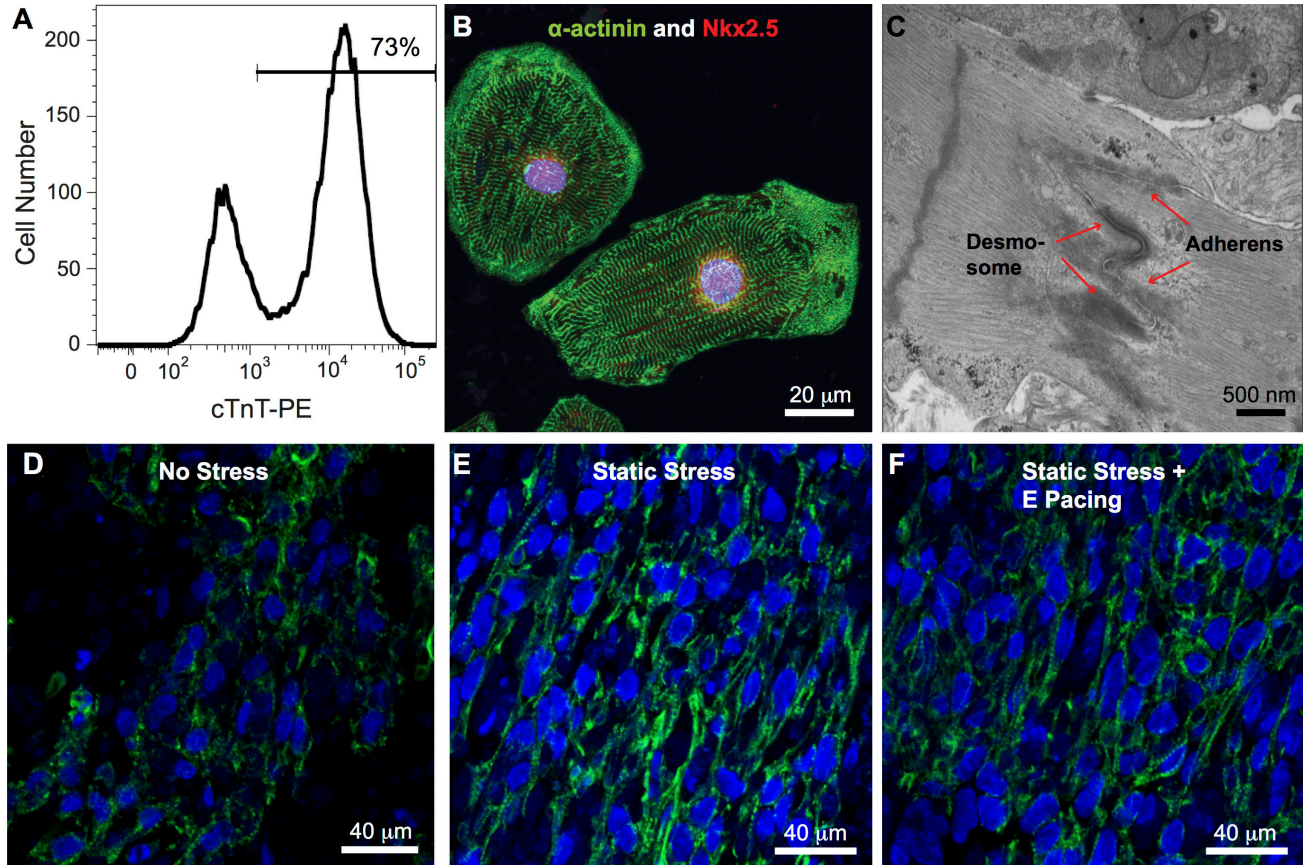


Figure 1.

Generation of high purity human iPS cell-derived constructs. A, Human cardiomyocytes were generated from the IMR90-iPS cell line at a purity of over 70% by cardiac troponin T (cTnT) flow cytometric analysis. B, The cardiomyocytes displayed robust sarcomeric organization by α -actinin immunostaining (green), as well as nuclear expression of the cardiomyocyte transcription factor Nkx2.5 (red). C, Primitive intercalated disc-like structures containing fascia adherens junctions and desmosomes (arrow) are present in the engineered heart tissue. Nuc: nucleus, Glyc: glycogen. Immunofluorescent staining for cardiac troponin T of iPS cells-derived human bioengineered cardiac tissues under NS, D, and SS, E, and SE, F, conditioning, shows greater alignment in the SS and SE tissue constructs.

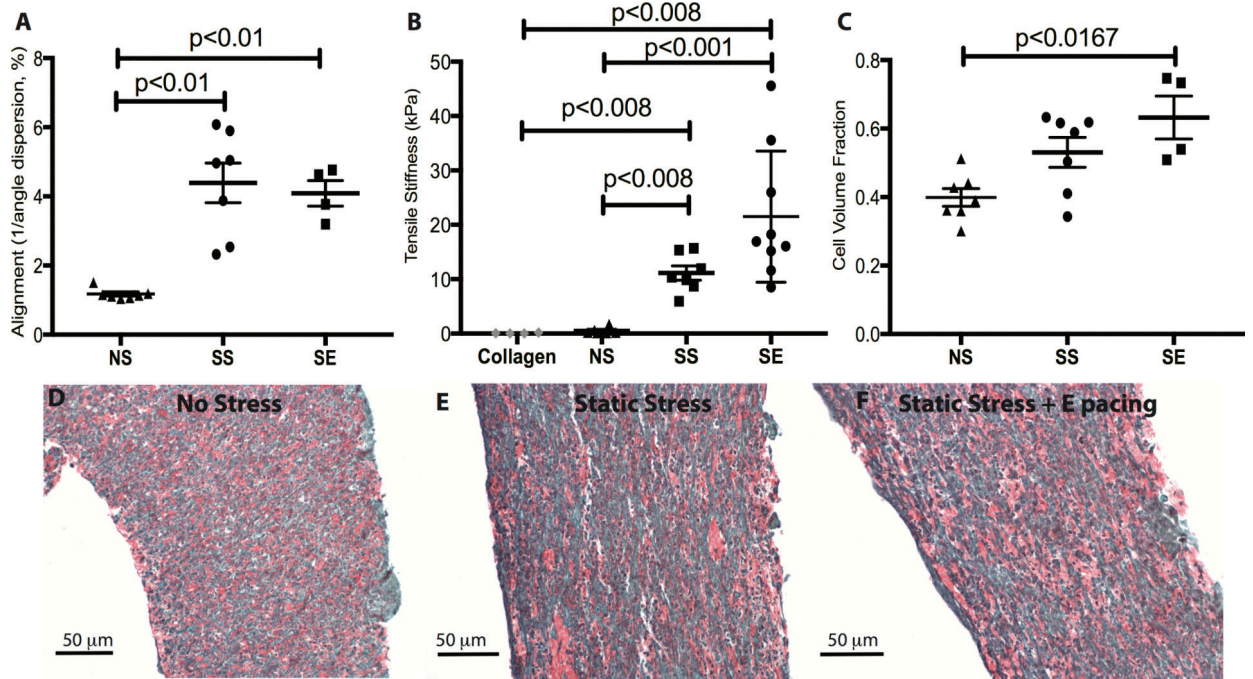


Figure 2.

Characterization of cell alignment and matrix remodeling. A, Constructs exposed to stress conditioning demonstrated significantly increased cell alignment compared to constructs without stress conditioning. Electrical pacing along with stress conditioning did not further promote the cell alignment. $n=7$ for NS, $n=7$ for SS, and $n=4$ for SE. B, The passive stiffness of constructs was measured by stretching constructs incrementally to 125% of slack length. Tensile stiffness was estimated from the slope of passive stress-strain relationship. The tensile stiffness of cell-free collagen matrix is 0.079 ± 0.041 kPa. Addition of cells increased the stiffness ~ 7 -fold, stress conditioning by a further ~ 20 -fold, and electrical pacing by an additional ~ 2 -fold (NS: 0.47 ± 0.22 kPa; SS: 11.13 ± 1.17 kPa; SE: 21.51 ± 4.02 kPa.). $n=6$ for NS, $n=7$ for SS, and $n=9$ for SE. C, Electrical pacing promotes ECM remodeling by increasing the cell volume fraction within the constructs (NS vs SS, $p=0.0728$, NS vs SE, $p=0.0121$, SS vs SE, $P=0.3$). $n=7$ for NS, $n=7$ for SS, and $n=4$ for SE. D, E, and F, are representative Sirius Red/Fast Green stains of NS, SS and SE, respectively.

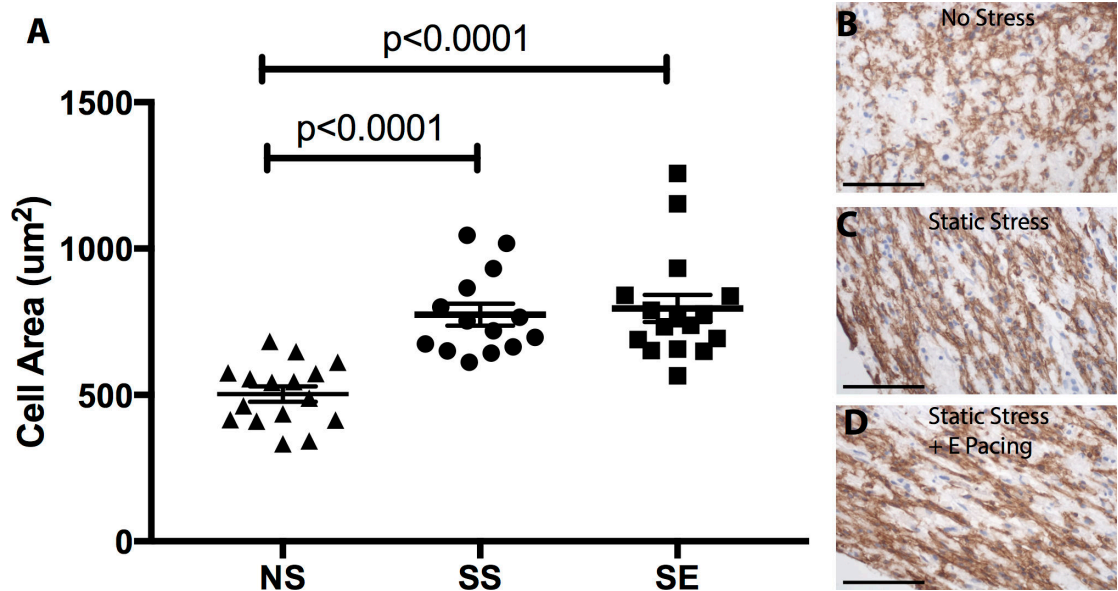


Figure 3. Stress conditioning increases cardiomyocyte hypertrophy. A, MYH7 positive area was measured to determine cardiomyocyte size from constructs in the different conditioning regimes. Cardiomyocyte size increased ~50% from NS vs. SS constructs, with no further increase in the ES group. (NS to SS, NS to SE, $p < 0.0001$) B, C, and D, show MYH7 positive cells in constructs from NS, SS, and SE, respectively. $n = 16$ for NS, $n = 14$ for SS, and $n = 14$ for SE. Hematoxylin counterstain denotes nuclei. The scale bar is $50 \mu\text{m}$.

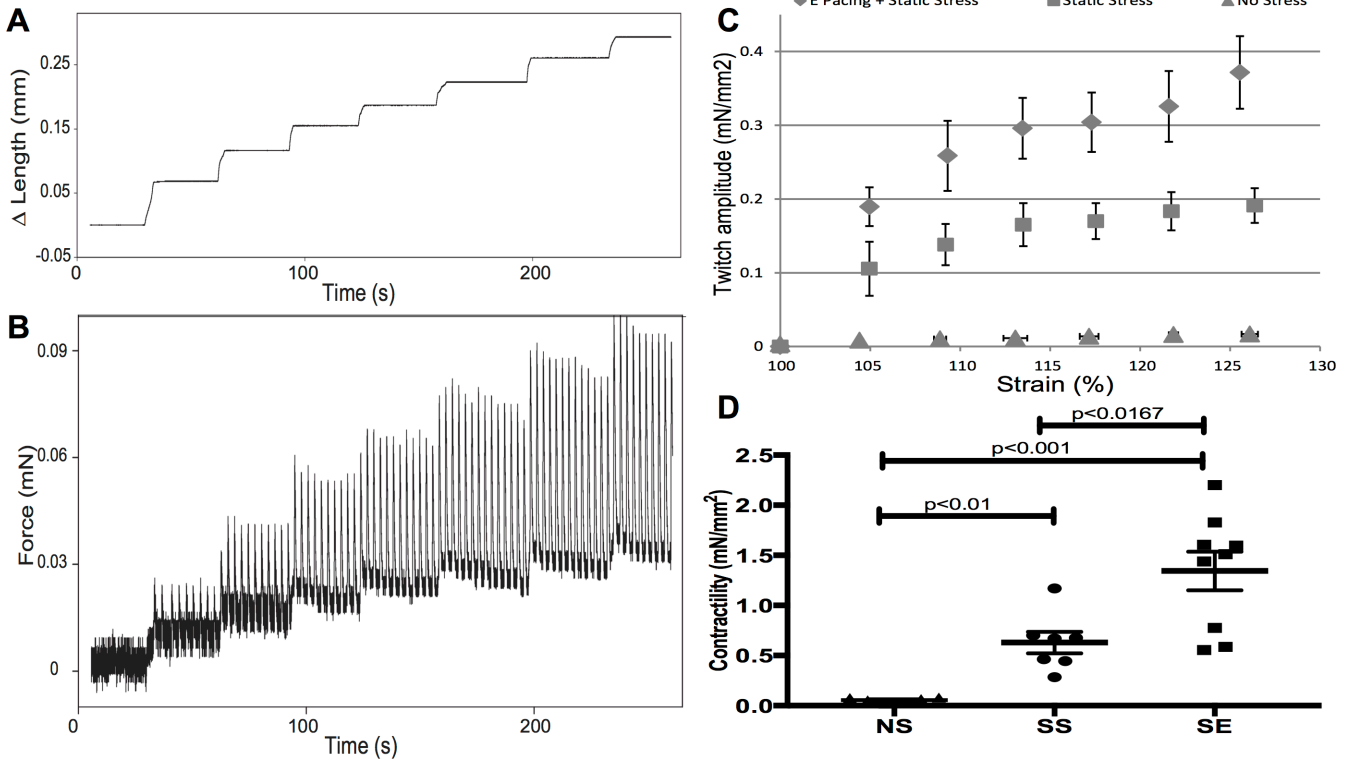


Figure 4. Stress conditioning and electrical stimulation increase contractility. Representative length (A) and force (B) traces demonstrate the response of a spontaneously contracting cardiac tissue construct to a series of stretches up to 125% of slack length. The amplitude of the isometric twitch force increases with increasing preparation length, in accordance with the Frank-Starling mechanism. C, Isometric twitch force amplitude measured at different preparation lengths is enhanced by 2 weeks of SS conditioning (triangles) in comparison to NS conditioning (triangles). Addition of electrical stimulation (diamonds) further increases contractility as show in (D). D, Contractility of constructs from the 3 stimulation conditions. Contractility is measured from the slope of the twitch force-strain curve, which is the active force development. The contractility of no stress constructs is 0.055 ± 0.009 mN/mm². Stress conditioning promotes the contractility 10-fold (0.63 ± 0.10 mN/mm²) and addition of electrical pacing further enhances force development another 2-fold (1.34 ± 0.19 mN/mm²). NS vs SS: $p < 0.01$; SS vs SE: $p < 0.01$. $n = 6$ for NS, $n = 7$ for SS, and $n = 9$ for SE.

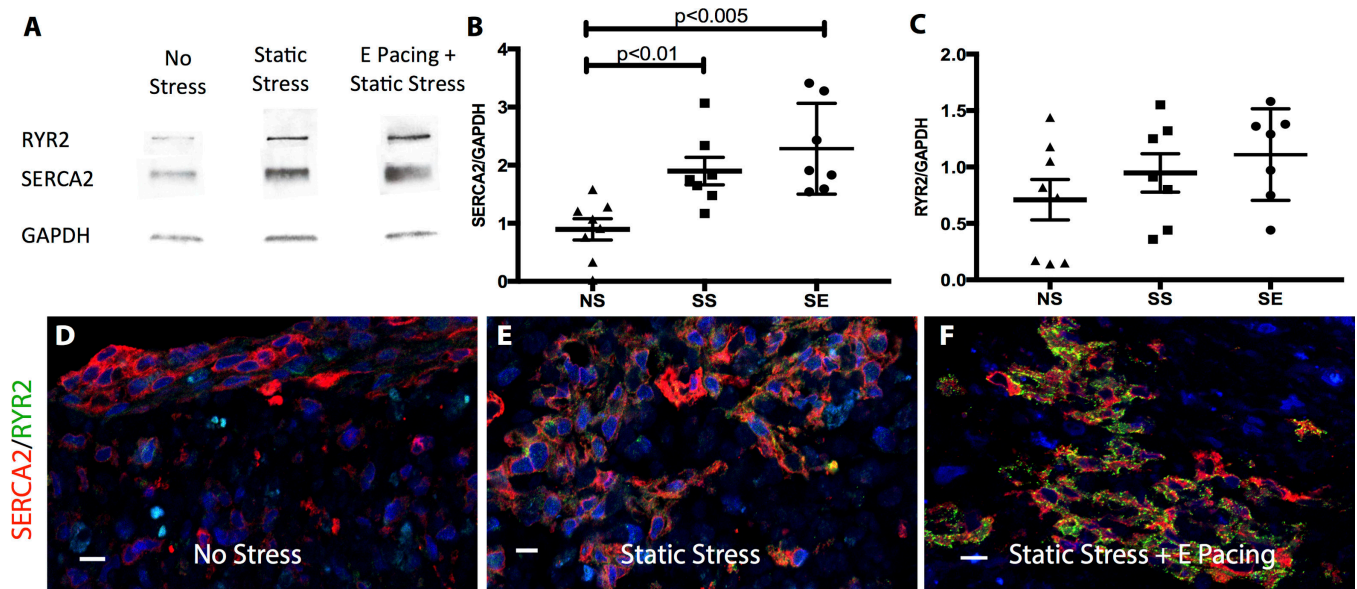


Figure 5.

Increase in calcium handling protein expression by stress conditioning and electrical stimulation. A, Western blot of SR-related proteins, SERCA2 and RYR2, from constructs subjected to different conditioning regimes. B&C, Dot plot of quantified western blot data. Data are normalized to internal control (GAPDH). B, Compared to the NS control, SS conditioned constructs increase SERCA2 expression by 2-fold (NS vs SS, $p < 0.01$) and SE-conditioned constructs by 2.5-fold (NS vs SE, $p < 0.005$). C, An increasing RYR2 expression trend is observed from NS to SE constructs but did not reach statistical significance. $n=8$ for NS, $n=7$ for SS, and $n=7$ for SE. Representative immunostaining images of engineered cardiac tissues stained with SERCA2 (red) and RYR2 (green) from NS (D), SS (E) and SE (F) conditionings. The scale bar is 10 μm .

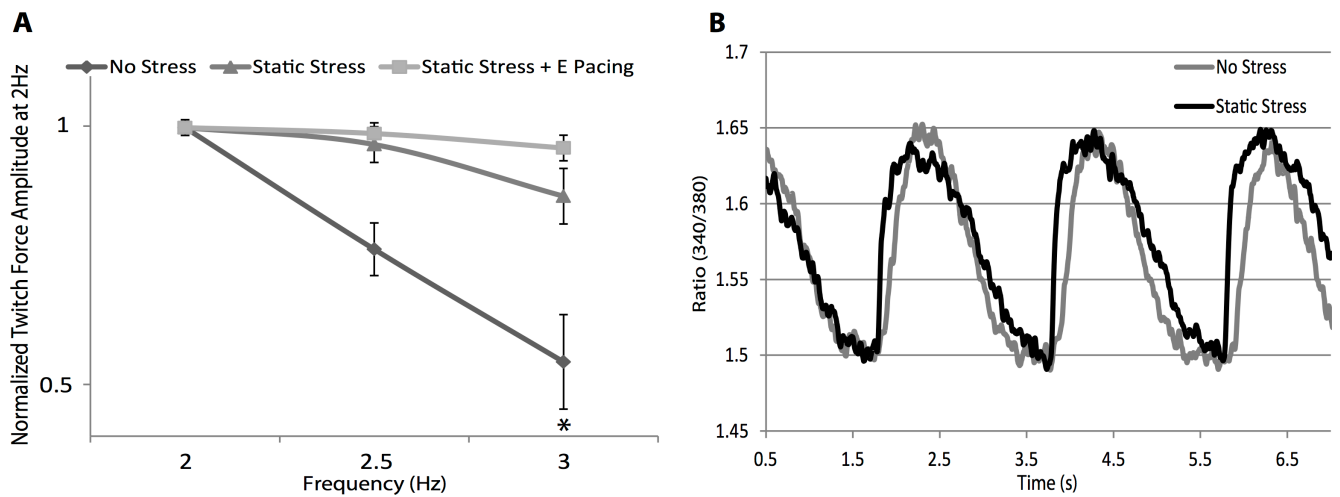


Figure 6.

Force frequency relationship and calcium transient characteristics of engineered cardiac tissues. A, Engineered cardiac tissues were subjected to 2, 2.5, and 3 Hz pacing and the twitch amplitude at 2 Hz was used to normalize other pacing frequencies. Due to immature development of SR, the force frequency relations of these constructs are negative, but static stress and electrical pacing pre-conditioning were able to mitigate the effect (NS $p=0.0047$ for 2 Hz vs 3 Hz; SS $p=0.09$ for 2 Hz vs 3 Hz; SE $p=0.8$ for 2 Hz vs 3 Hz). $n=5$ for NS, $n=11$ for SS, and $n=4$ for SE. B, Representative calcium transient from NS (gray) and SS (black)-conditioned constructs under 0.5 Hz pacing.